Mathematical Geology, Vol. 37, No. 4, May 2005 (© 2005)
DOI: 10.1007/s11004-005-5953-3

Artificial Lineaments in Digital Terrain Modelling: Can Operators of Topographic Variables Cause Them?[1]

Igor V. Florinsky[2,3,4]

Digital terrain modeling is widely used in geological studies. In some cases, orthogonal and diagonal linear patterns appear on maps of local topographic variables. These patterns may be both portrayals of geological structures and artefacts. Some researchers speculated that possible anisotropy of operators of local topographic variables might be a cause of these artefacts. Using a principle for testing derivative operators in image processing, we gave proof to isotropy (rotation invariability) of operators of a majority of local topographic attributes of the complete system of curvatures (i.e., slope gradient, horizontal curvature, vertical curvature, mean curvature, Gaussian curvature, accumulation curvature, ring curvature, unsphericity curvature, difference curvature, minimum curvature, maximum curvature, horizontal excess curvature, and vertical excess curvature). Rotating an elevation function about z-axis and then applying these operators cannot lead to variations in both values of the topographic variables and patterns in their maps, comparing with results of applying these operators to an unrotated elevation function. This demonstrates that linear artefacts with preferable directions in maps of the topographic attributes specified cannot be caused by intrinsic properties of their operators. Other possible sources for false linear patterns in maps of topographic variables are briefly discussed: (a) errors in the compilation of digital elevation models (DEMs), (b) grid geometry of digital terrain models (DTMs), (c) errors in DEM interpolation, (d) imperfection of algorithms for DTM derivation, and (e) aliasing errors.

KEY WORDS: curvature, surface, digital terrain modeling, derivative, lineament, artefact.

INTRODUCTION

It is well known that topography is one of the key indicators of geological structure at wide range of scales. For the last four decades, this has led to widespread use of digital terrain modeling in geology. Digital terrain modeling is a system of quantitative methods to model and analyze the land surface and relationships between the topography and geological, hydrological, biological, and

[1]Received 18 February 2004; accepted 23 September 2004.
[2]DTM Lab, 1026–110 Adamar Road, Winnipeg, Manitoba R3T 3M3, Canada.
[3]Institute of Mathematical Problems of Biology, Russian Academy of Sciences, Pushchino, Moscow Region 142292, Russia.
[4]Present address: Solomenskaya ul., dom 41, korpus 2, kv. 117, Kiev 03141, Ukraine; e-mail: iflorinsky@yahoo.ca

Table 1. Definitions of Local Topographic Variables the Complete System of Curvatures (Shary, 1995)

Variable and unit	Definition
Slope gradient (G) ($^\circ$)	An angle between a tangent plane and a horizontal one at a given point on the land surface.
Slope aspect (A) ($^\circ$)	An angle clockwise from the direction of y-axis to a projection of an external normal vector to a horizontal plane at a given point on the land surface.
Vertical curvature (k_v) (m^{-1})	A curvature of a normal section of the land surface by a plane, including gravity acceleration vector at a given point.
Horizontal curvature (k_h) (m^{-1})	A curvature of a normal section of the land surface which is orthogonal to the section of vertical curvature at a given point on the land surface.
Gaussian curvature (K) (m^{-2})	A product of maximum curvature and minimum curvature.
Mean curvature (H) (m^{-1})	A half-sum of curvatures of two orthogonal normal sections of the land surface at a given point.
Difference curvature (E) (m^{-1})	A half-difference of vertical and horizontal curvatures.
Accumulation curvature (K_a) (m^{-2})	A product of vertical and horizontal curvatures.
Unsphericity curvature (M) (m^{-1})	A half-difference of maximum and minimum curvatures.
Ring curvature (K_r) (m^{-2})	A product of horizontal excess and vertical excess curvatures.
Horizontal excess curvature (k_he) (m^{-1})	A difference of horizontal and minimum curvatures.
Vertical excess curvature (k_ve) (m^{-1})	A difference of vertical and minimum curvatures.
Minimum curvature (k_min) (m^{-1})	A curvature of a normal section with the smallest value of curvature among all normal sections at a given point of the land surface.
Maximum curvature (k_max) (m^{-1})	A curvature of a normal section with the largest value of curvature among all normal sections at a given point of the land surface.

Note. Physical interpretations and examples of application of local topographic attributes can be found elsewhere (Florinsky, 1998b; Shary, Sharaya, and Mitusov, 2002).

anthropogenic components of the landscape (see reviews—Moore, Grayson, and Ladson, 1991; Florinsky, 1998b; Pike, 2000). In geology, digital terrain modeling can be used to study not only the land surface, but also surfaces of stratigraphic horizons or geological structures (McCullagh, 1988). By digital terrain models (DTMs) are meant digital representations of variables describing the topographic and geological surfaces; namely, digital elevation models (DEMs), digital models of local topographic variables (Tables 1 and 2) and other geomorphometric indices.

Table 2. Formalism of Local Topographic Variables (Shary, 1995; Shary, Sharaya, and Mitusov, 2002)

Variable and unit	Formula
Slope gradient (G) ($^\circ$)	$G = \arctan\sqrt{p^2+q^2}$
Slope aspect (A) ($^\circ$)	$A = \arctan\left(\frac{q}{p}\right)$
Horizontal curvature (k_h) (m^{-1})	$k_\mathrm{h} = -\frac{q^2r-2pqs+p^2t}{(p^2+q^2)\sqrt{1+p^2+q^2}}$
Vertical curvature (k_v) (m^{-1})	$k_\mathrm{v} = -\frac{p^2r+2pqs+q^2t}{(p^2+q^2)\sqrt{(1+p^2+q^2)^3}}$
Gaussian curvature (K) (m^{-2})	$K = k_\mathrm{min}k_\mathrm{max} = \frac{rt-s^2}{(1+p^2+q^2)^2}$
Mean curvature (H) (m^{-1})	$H = \frac{1}{2}(k_\mathrm{min}+k_\mathrm{max}) = \frac{1}{2}(k_\mathrm{h}+k_\mathrm{v}) = -\frac{(1+q^2)r-2pqs+(1+p^2)t}{2\sqrt{(1+p^2+q^2)^3}}$
Difference curvature (E) (m^{-1})	$E = \frac{1}{2}(k_\mathrm{v}-k_\mathrm{h}) = \frac{(q^2r-2pqs+p^2t)(1+p^2+q^2)-(p^2r+2pqs+q^2t)}{2(p^2+q^2)\sqrt{(1+p^2+q^2)^3}}$
Accumulation curvature (K_a) (m^{-2})	$K_\mathrm{a} = k_\mathrm{h}k_\mathrm{v} = \frac{(q^2r-2pqs+p^2t)(p^2r+2pqs+q^2t)}{[(p^2+q^2)(1+p^2+q^2)]^2}$
Unsphericity curvature (M) (m^{-1})	$M = \frac{1}{2}(k_\mathrm{max}-k_\mathrm{min}) = \sqrt{H^2-K}$
Ring curvature (K_r) (m^{-2})	$K_\mathrm{r} = k_\mathrm{he}k_\mathrm{ve} = M^2-E^2 = \left[\frac{(p^2-q^2)s-pq(r-t)}{(p^2+q^2)(1+p^2+q^2)}\right]^2$
Horizontal excess curvature (k_he) (m^{-1})	$k_\mathrm{he} = k_\mathrm{h}-k_\mathrm{min} = M-E$
Vertical excess curvature (k_ve) (m^{-1})	$k_\mathrm{ve} = k_\mathrm{v}-k_\mathrm{min} = M+E$
Minimum curvature (k_min) (m^{-1})	$k_\mathrm{min} = H-M$
Maximum curvature (k_max) (m^{-1})	$k_\mathrm{max} = H+M$

Note. $p = \frac{\partial z}{\partial x}$, $q = \frac{\partial z}{\partial y}$, $r = \frac{\partial^2 z}{\partial x^2}$, $s = \frac{\partial^2 z}{\partial x \partial y}$ and $t = \frac{\partial^2 z}{\partial y^2}$ for the elevation given by $z = f(x, y)$; x and y are Cartesian co-ordinates. p, q, r, s, and t can be calculated by various methods (see formalism elsewhere—Florinsky, 1998a). For example, in the Evans method, the following formulae are used to estimate p, q, r, s, and t at the point $(0, 0, z_5)$ of a 3×3 elevation submatrix $[(-w,w,z_1), (0,w,z_2), (w,w,z_3), (-w,0,z_4), (0, 0, z_5), (w,0, z_6), (-w,-w,z_7), (0, -w,z_8), (w,-w,z_9)]$ moved along a square-gridded DEM: $p = \frac{z_3+z_6+z_9-z_1-z_4-z_7}{6w}$, $q = \frac{z_1+z_2+z_3-z_7-z_8-z_9}{6w}$, $r = \frac{z_1+z_3+z_4+z_6+z_7+z_9-2(z_2+z_5+z_8)}{3w^2}$, $s = \frac{z_3+z_7-z_1-z_9}{4w^2}$, $t = \frac{z_1+z_2+z_3+z_7+z_8+z_9-2(z_4+z_5+z_6)}{3w^2}$.

To reveal folds, faults, and ring structures, two well-known mathematical procedures, trend-analysis and spatial filtering, have been frequently utilized to process both DEMs of land surface and DEMs of stratigraphic horizons (Robinson, Charlesworth, and Ellis, 1969; Gosteva, Patrakova, and Abramkina, 1983). Wladis (1999) applied a geophysical method of second derivative filtering to a land surface DEM for revealing geological lineaments.

There are approaches involving an analysis of digital models of geomorphometric indices derived from land surface DEMs, such as summit level, base level, and relative relief (highest altitude, lowest altitude, and difference between them for a given area, correspondingly). These digital models were used to reveal active tectonic structures (Ioffe and Kozhurin, 1997), to recognize palaeosurfaces (Johansson, 1999), to estimate seismic activity (Zamani and Hashemi, 2000), and to study the interaction between endo- and exogenic processes of orogenesis (Kühni and Pfiffner, 2001).

Digital reflectance mapping (hillshading) based on the processing of land surface DEMs is widely used to highlight topographically expressed geological structures (Chorowicz, Dhont, and Gündoğdu, 1999). Superposition of geological time data on hillshading maps can improve the perception of relationships between geological and geomorphic features (Vigil, Pike, and Howell, 2000). Three-dimensional simulation using DEMs of the land surface and geological surfaces is also commonly used to visualize clearly the structure of landscapes together with geological strata, and to measure parameters of geological objects (Morris, 1991).

Geological applications of local topographic variables (Tables 1 and 2) are less common. Belonin and Zhukov (1968) studied an uplift evolution analyzing level, direction and unevenness of stretching and bending of several conformable stratigraphic surfaces using their K, H, $k_{\min}$, and $k_{\max}$. Chorowicz and others (1989) developed a method to recognize lithological boundaries using G, A and drainage/divide lines derived from a land surface DEM. k_h and k_v of the land surface were used to reveal topographically expressed lineaments and ring structures (Florinsky, 1993), and to distinguish strike-slip, dip-slip, and reverse faults at a regional scale (Florinsky, 1996, 1998c). This method was also applied to reveal faults of several conformable stratigraphic horizons using DEMs of their surfaces (Florinsky, Grokhlina, and Mikhailova, 1995). Lisle (1994) used K of geological surfaces to analyze fracture densities and strains of individual structures. Samson and Mallet (1997) proposed using $k_{\min}$ and $k_{\max}$ of geological surfaces to highlight hidden folding and faulting zones. K_a and H of the land surface were applied to investigate relationships between sites of fault intersection and land surface zones of flow accumulation (Florinsky, 2000).

When DTMs of local topographic variables are used to reveal lineaments and faults, indicators of these structures are linear patterns in maps of these variables (Fig. 1). Every so often near-north-, near-west-, near-northeast-, and

near-northwest-striking linear patterns are observed in the maps. Although these orthogonal and diagonal lineaments can be a reflection of topographically expressed geological structures, they may also be artefacts. There are several possible causes of them (Florinsky, 1993): (a) the geometry of the DTM grid, (b) errors

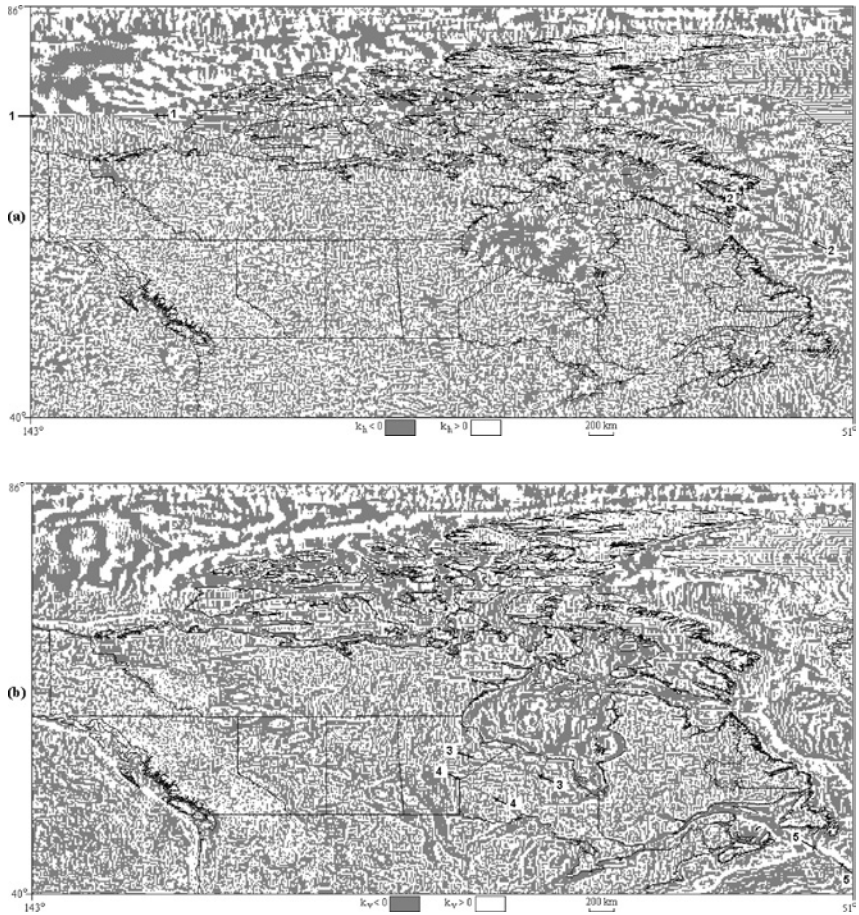

Figure 1. Canada and adjacent territories: maps of A, land surface k_h, and B, land surface k_v. These 10-arc-min gridded digital models of k_h and k_v each including 151,525 points were derived from a DEM by the method of Florinsky (1998c) using LandLord software (Florinsky, Grokhlina, and Mikhailova, 1995). The 10-arc-minute gridded DEM including 153,182 points was extracted from the ETOPO5 DEM (NOAA, 1988). Maps were visualized by ArcView GIS 3.0a (©1992–1997, ESRI). Lineaments are indicated by arrows: 1 is an example of artefacts due to errors of DEM compilation (see Results and Discussion for details), while 2, 3, 4, and 5 are examples of geological faults established earlier using conventional geological methods (Douglas, 1974; Sheridan, 1989).

in the DEM compilation, (c) errors in the DEM interpolation, (d) aliasing errors, (e) imperfection of algorithms for DTM derivation, and (f) anisotropy of operators of local topographic variables (see Results and Discussion for details). Orientation is an essential attribute of geological features, so possible false linear patterns on maps can lead to geological misinterpretation. To prevent this and to gain insight into methods and algorithms of digital terrain modeling, it is important to investigate causes responsible for artificial patterns of preferable direction in models and maps of topographic attributes. In this paper, we dwell on the question of whether operators of local topographic variables are isotropic.

It is common knowledge of the theory of image processing that derivative operators for transformation of two-dimensional signals may be isotropic and anisotropic (Rosenfeld and Kak, 1982). By isotropic operators are meant rotation invariants: rotating a function $z = f(x, y)$ by an angle φ about z-axis and then applying an operator Ω to $z = F(x', y')$ gives the same result as applying Ω to $z = f(x, y)$ and then rotating a result by the angle φ about z-axis; $F(x', y') = f(x, y)$, x, y and x', y' are the unrotated and the rotated Cartesian co-ordinates, correspondingly. An operator is anisotropic if this condition is not met. An example of isotropic operators is the Laplacian, while anisotropic operators are typified by compass operators measuring gradients in several directions.

Deriving a digital model of a local topographic variable l from a DEM by a related formula (Table 2) can be considered as applying an operator Ω of the variable l to an elevation function z. The operator Ω transforms the elevation function $z = f(x, y)$ into the function of the local topographic variable $l = \psi(x, y)$, or, what is the same—the DEM into the digital model of l.

Local topographic variables are functions of the first and second partial derivatives of elevation (Table 2). It would be reasonable to suggest that operators of these variables may also be isotropic or anisotropic. In spite of the importance of this question to digital terrain modeling, previous statements about rotation invariability of local topographic attributes were done without proof (Shary, Sharaya, and Mitusov, 2002). Indeed, it may be self-evident that local topographic variables, except A, are independent of the orientation of x- and y-axes if one will take a closer look at their definitions (Table 1). All these attributes, except A, are associated with directions related to intristic properties of the surface rather than orientation of the co-ordinate axes. However, although DTM-users are acquainted with physical interpretations of topographic attributes, they are usually not familiar with differential geometry. The author's experience shows that some researchers prefer to ascribe an occurrence of linear patterns of preferable directions in maps of local topographic variables to probable anisotropic properties of their operators, and to ignore arguments against this conclusion following from definitions of these variables (Table 1). This suggests that there is a need to present an alternative proof of the isotropy for operators of local topographic variables. This is the objective of the paper.

MATHEMATICAL TREATMENT

To prove the isotropy of operators of local topographic variables of the complete system of curvatures (Tables 1 and 2), we applied a principle for testing derivative operators in image processing (Rosenfeld and Kak, 1982, p. 238).

First, let us derive the first and second partial derivatives of $z = F(x', y')$, that is, p', q', r', s', and t', given in terms of the first and second partial derivatives of $z = f(x, y)$, that is, p, q, r, s, and t (Table 2). After applying the chain-rule of a change of the independent variables in differentiation of compound functions (Fikhtengolts, 1966; Courant and John, 1974), simple algebraic operations, and substitutions of the well-known expressions of co-ordinate rotation

$$x = x' \cos \varphi - y' \sin \varphi, \tag{1}$$

$$y = x' \sin \varphi + y' \cos \varphi, \tag{2}$$

we obtained the following formulae:

$$p' = \frac{\partial z}{\partial x'} = \frac{\partial z}{\partial x}\frac{\partial x}{\partial x'} + \frac{\partial z}{\partial y}\frac{\partial y}{\partial x'} = p \cos \varphi + q \sin \varphi \tag{3}$$

$$q' = \frac{\partial z}{\partial y'} = \frac{\partial z}{\partial x}\frac{\partial x}{\partial y'} + \frac{\partial z}{\partial y}\frac{\partial y}{\partial y'} = q \cos \varphi - p \sin \varphi \tag{4}$$

$$\begin{aligned} r' = \frac{\partial^2 z}{\partial x'^2} &= \frac{\partial}{\partial x'}\left(\frac{\partial z}{\partial x}\frac{\partial x}{\partial x'} + \frac{\partial z}{\partial y}\frac{\partial y}{\partial x'}\right) = \frac{\partial z}{\partial x}\frac{\partial^2 x}{\partial x'^2} \\ &+ \frac{\partial x}{\partial x'}\frac{\partial}{\partial x'}\left(\frac{\partial z}{\partial x}\right) + \frac{\partial z}{\partial y}\frac{\partial^2 y}{\partial x'^2} + \frac{\partial y}{\partial x'}\frac{\partial}{\partial x'}\left(\frac{\partial z}{\partial y}\right) = \frac{\partial z}{\partial x}\frac{\partial^2 x}{\partial x'^2} + \frac{\partial z}{\partial y}\frac{\partial^2 y}{\partial x'^2} \\ &+ \frac{\partial x}{\partial x'}\left(\frac{\partial^2 z}{\partial x^2}\frac{\partial x}{\partial x'} + \frac{\partial^2 z}{\partial x \partial y}\frac{\partial y}{\partial x'}\right) + \frac{\partial y}{\partial x'}\left(\frac{\partial^2 z}{\partial x \partial y}\frac{\partial x}{\partial x'} + \frac{\partial^2 z}{\partial y^2}\frac{\partial y}{\partial x'}\right) \\ &= \frac{\partial z}{\partial x}\frac{\partial^2 x}{\partial x'^2} + \frac{\partial z}{\partial y}\frac{\partial^2 y}{\partial x'^2} + \frac{\partial^2 z}{\partial x^2}\left(\frac{\partial x}{\partial x'}\right)^2 + 2\frac{\partial^2 z}{\partial x \partial y}\frac{\partial x}{\partial x'}\frac{\partial y}{\partial x'} + \frac{\partial^2 z}{\partial y^2}\left(\frac{\partial y}{\partial x'}\right)^2 \\ &= r \cos^2 \varphi + 2s \cos \varphi \sin \varphi + t \sin^2 \varphi \end{aligned} \tag{5}$$

$$\begin{aligned} s' = \frac{\partial^2 z}{\partial x' \partial y'} &= \frac{\partial}{\partial x'}\left(\frac{\partial z}{\partial x}\frac{\partial x}{\partial y'} + \frac{\partial z}{\partial y}\frac{\partial y}{\partial y'}\right) = \frac{\partial z}{\partial x}\frac{\partial^2 x}{\partial x' \partial y'} + \frac{\partial x}{\partial y'}\frac{\partial}{\partial x'}\left(\frac{\partial z}{\partial x}\right) \\ &+ \frac{\partial z}{\partial y}\frac{\partial^2 y}{\partial x' \partial y'} + \frac{\partial y}{\partial y'}\frac{\partial}{\partial x'}\left(\frac{\partial z}{\partial y}\right) = \frac{\partial z}{\partial x}\frac{\partial^2 x}{\partial x' \partial y'} + \frac{\partial z}{\partial y}\frac{\partial^2 y}{\partial x' \partial y'} \\ &+ \frac{\partial x}{\partial y'}\left(\frac{\partial^2 z}{\partial x^2}\frac{\partial x}{\partial x'} + \frac{\partial^2 z}{\partial x \partial y}\frac{\partial y}{\partial x'}\right) + \frac{\partial y}{\partial y'}\left(\frac{\partial^2 z}{\partial x \partial y}\frac{\partial x}{\partial x'} + \frac{\partial^2 z}{\partial y^2}\frac{\partial y}{\partial x'}\right) = \frac{\partial z}{\partial x}\frac{\partial^2 x}{\partial x' \partial y'} \end{aligned}$$

$$+\frac{\partial z}{\partial y}\frac{\partial^2 y}{\partial x'\partial y'}+\frac{\partial^2 z}{\partial x^2}\frac{\partial x}{\partial x'}\frac{\partial x}{\partial y'}+\frac{\partial^2 z}{\partial x\partial y}\left(\frac{\partial x}{\partial y'}\frac{\partial y}{\partial x'}+\frac{\partial x}{\partial x'}\frac{\partial y}{\partial y'}\right)+\frac{\partial^2 z}{\partial y^2}\frac{\partial y}{\partial x'}\frac{\partial y}{\partial y'}$$
$$=(t-r)\cos\varphi\sin\varphi+s(\cos^2\varphi-\sin^2\varphi) \tag{6}$$

$$t'=\frac{\partial^2 z}{\partial y'^2}=\frac{\partial}{\partial y'}\left(\frac{\partial z}{\partial x}\frac{\partial x}{\partial y'}+\frac{\partial z}{\partial y}\frac{\partial y}{\partial y'}\right)=\frac{\partial z}{\partial x}\frac{\partial^2 x}{\partial y'^2}+\frac{\partial x}{\partial y'}\frac{\partial}{\partial y'}\left(\frac{\partial z}{\partial x}\right)$$
$$+\frac{\partial z}{\partial y}\frac{\partial^2 y}{\partial y'^2}+\frac{\partial y}{\partial y'}\frac{\partial}{\partial y'}\left(\frac{\partial z}{\partial y}\right)=\frac{\partial z}{\partial x}\frac{\partial^2 x}{\partial y'^2}+\frac{\partial z}{\partial y}\frac{\partial^2 y}{\partial y'^2}$$
$$+\frac{\partial x}{\partial y'}\left(\frac{\partial^2 z}{\partial x^2}\frac{\partial x}{\partial y'}+\frac{\partial^2 z}{\partial x\partial y}\frac{\partial y}{\partial y'}\right)+\frac{\partial y}{\partial y'}\left(\frac{\partial^2 z}{\partial x\partial y}\frac{\partial x}{\partial y'}+\frac{\partial^2 z}{\partial y^2}\frac{\partial y}{\partial y'}\right)$$
$$=\frac{\partial z}{\partial x}\frac{\partial^2 x}{\partial y'^2}+\frac{\partial z}{\partial y}\frac{\partial^2 y}{\partial y'^2}+\frac{\partial^2 z}{\partial x^2}\left(\frac{\partial x}{\partial y'}\right)^2+2\frac{\partial^2 z}{\partial x\partial y}\frac{\partial x}{\partial y'}\frac{\partial y}{\partial y'}+\frac{\partial^2 z}{\partial y^2}\left(\frac{\partial y}{\partial y'}\right)^2$$
$$=r\sin^2\varphi-2s\cos\varphi\sin\varphi+t\cos^2\varphi \tag{7}$$

As $p\neq p'$, $q\neq q'$, $r\neq r'$, $s\neq s'$, and $t\neq t'$, these partial differential operators are not rotation invariants.

Second, let us define G, A, k_{h}, k_{v}, and K (Table 2) for the case of rotated Cartesian co-ordinates, that is, in terms of p', q', r', s', and t' [Eqs. (3)–(7)]. After substitutions and simple algebraic operations, we obtained the formulae:

$$G'=\arctan\sqrt{p'^2+q'^2}=\arctan\sqrt{(p\cos\varphi+q\sin\varphi)^2+(q\cos\varphi-p\sin\varphi)^2}$$
$$=\arctan\sqrt{p^2(\cos^2\varphi+\sin^2\varphi)+q^2(\cos^2\varphi+\sin^2\varphi)}=\arctan\sqrt{p^2+q^2} \tag{8}$$

$$A'=\arctan\left(\frac{q'}{p'}\right)=\arctan\left(\frac{q\cos\varphi-p\sin\varphi}{p\cos\varphi+q\sin\varphi}\right) \tag{9}$$

$$k'_{\mathrm{h}}=-\frac{q'^2r'-2p'q's'+p'^2t'}{(p'^2+q'^2)\sqrt{1+p'^2+q'^2}}$$
$$=\Big\{-(q\cos\varphi-p\sin\varphi)^2(r\cos^2\varphi+2s\cos\varphi\sin\varphi+t\sin^2\varphi)$$
$$-2(p\cos\varphi+q\sin\varphi)(q\cos\varphi-p\sin\varphi)\{(t-r)\cos\varphi\sin\varphi+s(\cos^2\varphi$$
$$-\sin^2\varphi)\}+(p\cos\varphi+q\sin\varphi)^2(r\sin^2\varphi-2s\cos\varphi\sin\varphi+t\cos^2\varphi)\Big\}\Big/$$
$$\Big\{[(p\cos\varphi+q\sin\varphi)^2+(q\cos\varphi-p\sin\varphi)^2]$$
$$\times\sqrt{1+(p\cos\varphi+q\sin\varphi)^2+(q\cos\varphi-p\sin\varphi)^2}\Big\}$$

$$= -\frac{q^2 r - 2pqs + p^2 t}{(p^2 + q^2)\sqrt{1 + p^2 + q^2}} \tag{10}$$

$$\begin{aligned} k'_{\mathrm{v}} &= -\frac{p'^2 r' + 2p'q's' + q'^2 t'}{(p'^2 + q'^2)\sqrt{(1 + p'^2 + q'^2)^3}} \\ &= \{ -(p\cos\varphi + q\sin\varphi)^2 (r\cos^2\varphi + 2s\cos\varphi\sin\varphi + t\sin^2\varphi) \\ &\quad + 2(p\cos\varphi + q\sin\varphi)(q\cos\varphi - p\sin\varphi)\{(t-r)\cos\varphi\sin\varphi + s(\cos^2\varphi \\ &\quad - \sin^2\varphi)\} + (q\cos\varphi - p\sin\varphi)^2 (r\sin^2\varphi - 2s\cos\varphi\sin\varphi + t\cos^2\varphi)\} / \\ &\quad \{ [(p\cos\varphi + q\sin\varphi)^2 + (q\cos\varphi - p\sin\varphi)^2] \\ &\quad \times\sqrt{[1 + (p\cos\varphi + q\sin\varphi)^2 + (q\cos\varphi - p\sin\varphi)^2]^3} \} \\ &= -\frac{p^2 r + 2pqs + q^2 t}{(p^2 + q^2)\sqrt{(1 + p^2 + q^2)^3}} \end{aligned} \tag{11}$$

$$\begin{aligned} K' &= \frac{r't' - s'^2}{(1 + p'^2 + q'^2)^2} \\ &= \{(r\cos^2\varphi + 2s\cos\varphi\sin\varphi + t\sin^2\varphi)(r\sin^2\varphi - 2s\cos\varphi\sin\varphi \\ &\qquad + t\cos^2\varphi) - \{(t-r)\cos\varphi\sin\varphi + s(\cos^2\varphi - \sin^2\varphi)\}^2\} / \\ &\qquad \{[1 + (p\cos\varphi + q\sin\varphi)^2 + (q\cos\varphi - p\sin\varphi)^2]^2\} \\ &= \frac{rt - s^2}{(1 + p^2 + q^2)^2} \end{aligned} \tag{12}$$

Comparing the formalism of G', k'_{h}, k'_{v}, A' and K' for the rotated co-ordinates [Eqs. (8)–(12)] with the corresponding formalism for the unrotated co-ordinates (Table 2), it is possible to see that $G' = G$, $A' \neq A$, $k'_{\mathrm{h}} = k_{\mathrm{h}}$, $k'_{\mathrm{v}} = k_{\mathrm{v}}$, and $K' = K$. These mean that operators of G, k_{h}, k_{v}, and K are isotropic, while the operator of A is anisotropic.

H, E, and K_{a} can be expressed by the combinations of k_{h} and k_{v} (Table 2). Since operators of k_{h} and k_{v} are isotropic [Eqs. (10) and (11)], operators of H, E, and K_{a} are isotropic too:

$$H' = \frac{1}{2}(k'_{\mathrm{h}} + k'_{\mathrm{v}}) = \frac{1}{2}(k_{\mathrm{h}} + k_{\mathrm{v}}) \tag{13}$$

$$E' = \frac{1}{2}(k'_{\mathrm{v}} - k'_{\mathrm{h}}) = \frac{1}{2}(k_{\mathrm{v}} - k_{\mathrm{h}}) \tag{14}$$

$$K'_{\mathrm{a}} = k'_{\mathrm{h}} k'_{\mathrm{v}} = k_{\mathrm{h}} k_{\mathrm{v}} \tag{15}$$

M can be expressed by the combination of K and H (Table 2). Since their operators are rotation invariants [Eqs. (12) and (13)], so the operator of M is also a rotation invariant:

$$M' = \sqrt{H'^2 - K'} = \sqrt{H^2 - K} \tag{16}$$

K_r, k_{he}, k_{ve} can be expressed by the combinations of M and E (Table 2), while k_{min} and k_{max} can be expressed by the combinations of M and H (Table 2). As operators of H, E, and M are isotropic [Eqs. (13), (14), and (16)], so operators of K_r, k_{he}, k_{ve}, k_{min}, and k_{max} are isotropic too:

$$K'_r = M'^2 - E'^2 = M^2 - E^2 \tag{17}$$

$$k'_{he} = M' - E' = M - E \tag{18}$$

$$k'_{ve} = M' + E' = M + E \tag{19}$$

$$k'_{min} = H' - M' = H - M \tag{20}$$

$$k'_{max} = H' + M' = H + M \tag{21}$$

RESULTS AND DISCUSSION

We proved that operators of all local topographic variables of the complete system of curvatures, except A, are isotropic. This means that (a) rotating an elevation function about z-axis and then applying operators of G, k_h, k_v, H, K, K_a, K_r, M, E, k_{min}, k_{max}, k_{he}, k_{ve}, and any of their linear transformations cannot lead to variations in both values of the variables and patterns on their maps, comparing with results of applying these operators to an unrotated elevation function, and (b) application of these operators to DEMs cannot be responsible for the occurrence of artificial lineaments of preferable orientations in DTMs and maps derived.

Operators of A and its linear transformations are not rotation invariants. Rotating an elevation function about z-axis and then applying of the operator of A will lead to variations in both the A values and patterns in A maps, comparing with results of applying the operator to an unrotated elevation function. It is notable that, from a formal point of view, this is true for nonspecial points of a surface only, that is, points marked by $p^2 + q^2 \neq 0$, or $G > 0$. For special points of a surface, that is, $p^2 + q^2 = 0$, or $G = 0$, the operator of A might be considered as isotropic. However, this is meaningless: A cannot be defined for special points per se, since the gravity does not mark any direction there (Shary, 1995).

These results were expected as they follow from mathematical definitions of local topographic variables (Table 1).

To avoid misunderstanding, we should note that a rotation of a regular grid, wherein elevations are interpolated and/or topographic variables are calculated,

relative to an initial (irregular) DEM grid leads inevitably to changes of both values in DTMs and patterns in maps obtained. However, these effects are connected with discretization errors of an elevation function due to displacement of a DEM grid in its rotation, regardless to isotropy or anisotropy of an operator applied (see details elsewhere—Florinsky, 2002).

We presented the proof of isotropy for operators of local topographic variables of the complete system of curvatures (Shary, 1995) using their rigorous formula (Table 2). Sometimes, researchers use simplified versions of these expressions. To check isotropy of simplified operators as well as operators of other morphometric indices used in geosciences, one may apply the principle described in this paper.

Other Causes for Lineaments on Maps of Local Topographic Variables

Let us briefly review other causes for linear patterns on maps of local topographic variables (Florinsky, 1993).

Natural Orientation of Landform

It has been found that a considerable portion of topographically expressed fractured zones, faults, and lineaments of a tectonic origin are marked by near-north, near-west, near-northeast, and near-northwest orientations (Katterfeld and Charushin, 1973). This phenomenon manifests itself at a wide range of scales on the Earth and other terrestrial planets (Fig. 1). Assuming the absence of artefacts, this natural topographic anisotropy may be fully responsible for patterns of preferable orientations in maps of topographic attributes.

Geometry of DTM Grid

Digital terrain modeling usually involves a processing of a surface described at points arranged in a square or other regular grid. Obviously, visualization of results of DTM-based analysis, more or less, depends on geometry of this grid (e.g., orthogonal and diagonal directions). However, it is possible to ignore an influence of DTM grid geometry on the appearance of a map using DTMs marked by a sufficiently high resolution, when a grid raster does not impede visual perception of a user. It is also obvious that DTM grid geometry can influence not only a representation of results of DTM-based analysis but this analysis as well (e.g., DEM interpolation and DTM computations). These aspects are discussed below.

Errors in DEM Compilation

There are, at least, five groups of systematic errors of DEM compilation causing artificial linear patterns in maps and DTMs. First, there are linear artefacts

caused by banding, a by-product of photogrammetric generation of DEMs (Brown and Bara, 1994). Second, there are abrupt linear altitude steps resulting from processing an orthophoto as separate patches and subsequently joining them to assemble a DEM (Hunter and Goodchild, 1995). Third, artificial orthogonal linear scarps can be found in small-scale and global DEMs, the result of assembling several DEMs varying in origin and accuracy. A case in point is ETOPO5, 5-arc-min gridded global DEM (NOAA, 1988): particularly striking is the presence of orthogonal 'scarps' in Arctic regions (Fig. 1A). Fourth, artificial lineaments may be specifically inserted to a DEM. For example, the Canadian national DEM (Natural Resources Canada, 1997) includes 'sub-continental escarp' along 49°N because the Canadian/USA border is labeled as 0 m above sea level. Fifth, artificial lineaments may arise in detailed DEMs after digitizing man-made altitude differences located along some transport and industrial objects (roads, dams, etc.).

Errors in DEM Interpolation

It was found that interpolations of DEMs along a series of profiles of the four cardinal orientations, orthogonal, and diagonal, can lead to linear artefacts oriented in these directions (Wood and Fisher, 1993). Declercq (1996) carried out an assessment of spatial pattern visualization of non-topographic data using several interpolation methods, such as piecewise polynomials, quadratic and cubic splines, linear triangulation, proximation, distance weighting, and kriging. He demonstrated that for sparsely sampled areas, interpolation based on polynomials, splines, and linear triangulation can lead to production of artificial linear patterns of the cardinal orientations.

Pronounced linear artefacts, contour 'traces,' can be found in DEMs with 'enhanced' resolution. Their source is a wrong over-detailed grid size used for DEM interpolation. This situation was detailed and illustrated elsewhere (Florinsky, 2002).

Aliasing Errors (the Moiré Effect)

A cause of these artefacts well known in signal and image processing is the interference of two periodic structures (i.e., a function with actual periodic patterns and a discretization grid) using a wrong grid size to sample a periodic function (Rosenfeld and Kak, 1982). This may result in the occurrence of a system of artificial linear patterns of some orientation. In digital terrain modeling, the Moiré fringes may arise in studying a terrain with a well-marked spatial periodicity (e.g., dunes). As far as we know, the Moiré effect has yet to be analyzed in the context of digital terrain modeling.

It is obvious that linear artefacts of preferable orientations caused by DEM compilation and interpolation, and the Moiré effect can be propagated from DEMs

to secondary DTMs. Moreover, digital and visual manifestation of these artefacts can be increased in secondary DTMs derived from these DEMs using differentiation. This is connected with a well-known fact that differentiation of a function increases a noise manifestation (Florinsky, 2002). This may introduce a risk to DTM-based revealing of geological structures, since these approaches are based on a derivation of hillshading, k_h and k_v maps from DEMs using partial derivatives (Table 2).

Imperfection of Algorithms for DTM Derivation

Although a DEM may be free of linear artefacts, some secondary DTMs derived from the DEM may include them due to intrinsic properties of algorithms for DTM derivation. For example, some algorithms for derivation of drainage/divide networks from DEMs (i.e., 'streaming' and 'breadth-first search' algorithms) may produce pronounced parallel networks (Riazanoff, Cervelle, and Chorowicz, 1988; Liang and Mackay, 2000).

In the case of analytical description of a function, anisotropies of partial differential operators compensate each other once combined in operators of local topographic variables, except A. However, discrete computational procedures of digital terrain modeling usually involve approximations of partial derivatives by finite differences on regular grids (Table 2) rather than direct analytical calculations. A possible incomplete compensation of anisotropies of partial differential operators, especially with crude approximations, may be a problem. As far as we know, this issue has not been studied, although accuracy of several algorithms for approximation of p, q, r, s, and t was assessed (Florinsky, 1998a).

CONCLUSIONS

We proved that operators of local topographic variables of the complete system of curvatures, except A, are rotation invariants. Rotating an elevation function about z-axis and then applying these operators cannot lead to variations in both values of topographic variables and patterns in their maps, comparing with results of applying these operators to an unrotated elevation function. This demonstrates that linear artefacts of preferable directions in maps of G, k_h, k_v, H, K, K_a, K_r, M, E, k_{min}, k_{max}, k_{he}, and k_{ve} cannot be caused by intrinsic properties of their operators. However, the probability exists of retaining anisotropies of partial differential operators when combined in operators of local topographic variables, if partial differential operators are crudely approximated. This issue should be studied in the future.

We suppose that main sources of linear artefacts in DTMs and maps of local topographic variables are errors of DEM compilation and interpolation. However,

although errors of DEM compilation can lead to many false lineaments, they usually have a pronounced manifestation, and may be detected by a visual analysis (Hunter and Goodchild, 1995) and numerical procedures (Brown and Bara, 1994). In contrast, errors of DEM interpolation can introduce more problems for geological interpretations, especially in studies of geological surfaces: in this case, there is no an unambiguous and objective criterion to assess interpolation accuracy and fidelity of interpolated surfaces and/or revealed structures (McCullagh, 1988). This calls for further investigation of interpolation algorithms.

Study of errors leading to artificial lineaments in maps of topographic variables is an important issue in the context of expanding implementation of digital terrain modeling in geological studies. The expanding is connected with several factors. First, a physico-mathematical theory of a surface in gravity, the basis of digital terrain modeling, is being developed (Shary, 1995). Second, digital terrain modeling is characterized by relatively simple mathematics, algorithms, and software. Third, a raster format of DTMs is convenient to link them with geophysical and remotely sensed data. Fourth, methods of digital terrain modeling can be used at a broad range of spatial scales (Pike, 2000). Finally, global DEMs, such as ETOPO5 and GTOPO30 (NOAA, 1988; Gesch, Verdin, and Greenlee, 1999), as well as DEMs of some terrestrial planets and satellites (Smith and others, 1999) are available for an analysis.

REFERENCES

Belonin, M. D., and Zhukov, I. M., 1968, Geometrical properties of surfaces of the Alexeevskoye uplift, the Kuibyshev Region, *in* Romanova, M. A., ed., Problems of mathematical geology: Nauka, Leningrad, p. 194–207 (in Russian).

Brown, D. G., and Bara, T. J., 1994, Recognition and reduction of systematic error in elevation and derivative surfaces from 7.5-minute DEMs: Photogramm. Eng. Remote Sens., v. 60, no. 2, p. 189–194.

Chorowicz, J., Kim, J., Manoussis, S., Rudant, J., Foin, P., and Veillet, I., 1989, A new technique for recognition of geological and geomorphological patterns in digital terrain models: Remote Sens. Environ., v. 29, no. 3, p. 229–239.

Chorowicz, J., Dhont, D., and Gündoğdu, N., 1999, Neotectonics in the eastern North Anatolian fault region (Turkey) advocates crustal extension: Mapping from SAR ERS imagery and digital elevation model: J. Struct. Geol., v. 21, no. 5, p. 511–532.

Courant, R., and John, F., 1974, Introduction to calculus and analysis, Vol. 2: Wiley, New York, 954 p.

Declercq, F. A. N., 1996, Interpolation methods for scattered sample data: Accuracy, spatial patterns, processing time: Cartogr. Geogr. Inform. Syst., v. 23, no. 3, p. 128–144.

Douglas, R. J. W., 1974, Tectonics, *in* Fremlin, G., ed., The national atlas of Canada, 4th rev. edn.: Department of Energy, Mines and Resources and Information Canada, Ottawa, p. 29–30.

Fikhtengolts, G. M., 1966, A course in differential and integral calculus, 6th edn., Vol. 1: Nauka, Moscow, 607 p. (in Russian).

Florinsky, I. V., 1993, Analysis of digital elevation models for recognition of linear structures of the land surface: Unpublished Ph.D. Thesis, Institute of Soil Science and Photosynthesis, Russian Academy of Sciences, Pushchino, 133 p. (in Russian).

Florinsky, I. V., 1996, Quantitative topographic method of fault morphology recognition: Geomorphology, v. 16, no. 2, p. 103–119.

Florinsky, I. V., 1998a, Accuracy of local topographic variables derived from digital elevation models: Int. J. Geogr. Inform. Sci., v. 12, no. 1, p. 47–61.

Florinsky, I. V., 1998b, Combined analysis of digital terrain models and remotely sensed data in landscape investigations: Prog. Phys. Geogr., v. 22, no. 1, p. 33–60.

Florinsky, I. V., 1998c, Derivation of topographic variables from a digital elevation model given by a spheroidal trapezoidal grid: Int. J. Geogr. Inform. Sci., v. 12, no. 8, p. 829–852.

Florinsky, I. V., 2000, Relationships between topographically expressed zones of flow accumulation and sites of fault intersection: Analysis by means of digital terrain modelling: Environ. Modell. Softw., v. 15, no. 1, p. 87–100.

Florinsky, I. V., 2002, Errors of signal processing in digital terrain modelling: Int. J. Geogr. Inform. Sci., v. 16, no. 5, p. 475–501.

Florinsky, I. V., Grokhlina, T. I., and Mikhailova, N. L., 1995, LANDLORD 2.0: The software for analysis and mapping of geometrical characteristics of relief: Geodesiya Cartogr., no. 5, p. 46–51 (in Russian).

Gesch, D. B., Verdin, K. L., and Greenlee, S. K., 1999, New land surface digital elevation model covers the Earth: Eos, v. 80, no. 6, p. 69–70.

Gosteva, T. S., Patrakova, V. S., and Abramkina, V. A., 1983, Determination of laws controlling spatial distribution of ring structures on the basis of trend-analysis of the topography: Geol. Geophys., no. 8, p. 72–79 (in Russian, with English abstract).

Hunter, G. J., and Goodchild, M. F., 1995, Dealing with error in spatial databases: A simple case study: Photogramm. Eng. Remote Sens., v. 61, no. 5, p. 529–537.

Ioffe, A. I., and Kozhurin, A. I., 1997, Active tectonics and geoecological zoning of Moscow Region: Bull. Moscow Soc. Naturalists, Geol. Ser., v. 72, no. 5, p. 31–35 (in Russian, with English abstract).

Johansson, M., 1999, Analysis of digital elevation data for palaeosurfaces in south-western Sweden: Geomorphology, v. 26, no. 4, p. 279–295.

Katterfeld, G. N., and Charushin, G. V., 1973, General grid systems of planets: Mod. Geol., v. 4, no. 4, p. 253–287.

Kühni, A., and Pfiffner, O. A., 2001, The relief of the Swiss Alps and adjacent areas and its relation to lithology and structure: Topographic analysis from a 250-m DEM: Geomorphology, v. 41, no. 4, p. 285–307.

Liang, C., and Mackay, D. S., 2000, A general model of watershed extraction and representation using globally optimal flow paths and up-slope contributing areas: Int. J. Geogr. Inform. Sci., v. 14, no. 4, p. 337–358.

Lisle, R. J., 1994, Detection of zones of abnormal strains in structures using Gaussian curvature analysis: Am. Assoc. Petrol. Geol. Bull., v. 78, no. 12, p. 1811–1819.

McCullagh, M. J., 1988, Terrain and surface modelling systems: Theory and practice: Photogramm. Rec., v. 12, no. 72, p. 747–779.

Moore, I. D., Grayson, R. B., and Ladson, A. R., 1991, Digital terrain modelling: A review of hydrological, geomorphological and biological applications: Hydrol. Process., v. 5, no. 1, p. 3–30.

Morris, K., 1991, Using knowledge-base rules to map the three-dimensional nature of geological features: Photogramm. Eng. Remote Sens., v. 57, no. 9, p. 1209–1216.

Natural Resources Canada, 1997, Canadian Digital Elevation Data: Standards and Specifications: Centre for Topographic Information, Sherbrooke, 11 p.

NOAA, 1988, Digital Relief of the Surface of the Earth: NOAA, National Geophysical Data Center, Boulder, Data Announcement 88-MGG-02.

Pike, R. J., 2000, Geomorphometry—diversity in quantitative surface analysis: Prog. Phys. Geogr., v. 24, no. 1, p. 1–20.

Riazanoff, S., Cervelle, B., and Chorowicz, J., 1988, Ridge and valley line extraction from digital terrain models: Int. J. Remote Sens., v. 9, no. 6, p. 1175–1183.

Robinson, J. E., Charlesworth, H. A. K., and Ellis, M. J., 1969, Structural analysis using spatial filtering in Interior Plains of south-central Alberta: Am. Assoc. Petrol. Geologists Bull., v. 53, no. 11, p. 2341–2367.

Rosenfeld, A., and Kak, A. C., 1982, Digital picture processing, 2nd edn., Vol. 1: Academic Press, New York, 435 p.

Samson, P. P., and Mallet, J. L., 1997, Curvature analysis of triangulated surfaces in structural geology: Math. Geol., v. 29, no. 3, p. 391–412.

Shary, P. A., 1995, Land surface in gravity points classification by complete system of curvatures: Math. Geol., v. 27, no. 3, p. 373–390.

Shary, P. A., Sharaya, L. S., and Mitusov, A. V., 2002, Fundamental quantitative methods of land surface analysis: Geoderma, v. 107, no. 1–2, p. 1–32.

Sheridan, R. E., 1989, The Atlantic passive margin, *in* Bally, A. W., and Palmer, A. R., eds., The geology of North America—an overview: Geological Society of America, Boulder, p. 81–96.

Smith, D. E., Zuber, M. T., Solomon, S. C., Phillips, R. J., Head, J. W., Garvin, J. B., Banerdt, W. B., Muhleman, D. O., Pettengill, G. H., Neumann, G. A., Lemoine, F. G., Abshire, J. B., Aharonson, O., Brown, C. D., Hauck, S. A., Ivanov, A. B., Mcgovern, P. J., Zwally, H. J., and Duxbury, T. C., 1999, The global topography of Mars and implications for surface evolution: Science, v. 284, no. 5419, p. 1495–1503.

Vigil, J. F., Pike, R. J., and Howell, D. G., 2000, A Tapestry of Time and Terrain, USGS Geologic Investigations Series Map I-2720, scale 1:3 500 000: US Geological Survey.

Wladis, D., 1999, Automatic lineament detection using digital elevation models with second derivative filters: Photogramm. Eng. Remote Sens., v. 65, no. 4, p. 453–458.

Wood, J. D., and Fisher, P. F., 1993, Assessing interpolation accuracy in elevation models: IEEE Comp. Graph. Applic., v. 13, no. 2, p. 48–56.

Zamani, A., and Hashemi, N., 2000, A comparison between seismicity, topographic relief, and gravity anomalies of the Iranian Plateau: Tectonophysics, v. 327, no. 1–2, p. 25–36.